SCIENCE CHINA
Earth Sciences

• RESEARCH PAPER •

April 2011 Vol.54 No.4: 581–590
doi: 10.1007/s11430-011-4181-6

Sensitivity of simulated short-range high-temperature weather to land surface schemes by WRF

ZENG XinMin[1,2*], WU ZhiHuang[1], XIONG ShiYan[1], SONG Shuai[2], ZHENG YiQun[1] & LIU HuaQiang[1]

[1] *Institute of Meteorology, P.L.A. University of Science and Technology, Nanjing 211101, China;*
[2] *Key Laboratory of Regional Climate-Environment Research for Temperate East Asia (RCE-TEA), Chinese Academy of Sciences, Beijing 100029, China*

Received May 20, 2010; accepted November 4, 2010

The simulations of a heat wave occurring in southern Yangtze-Huaihe valley and southern China during late July, 2003 were conducted to examine the sensitivity of simulated surface air temperature (SAT) to different land surface schemes (LSSs) using the Weather Research and Forecasting Model (WRF) Version 2.2 in the short-range mode for 24-h integrations. Initial and boundary conditions employed a National Centers for Environmental Prediction (NCEP) analysis. The results showed that, overall, simulated high-temperature weather is sensitive to different LSSs. Large differences in simulated SAT intensity, threat score, and simulated error under different schemes are identified clearly. In addition, some systematic differences are also induced by the LSSs. In terms of threat score from the three LSSs, SLAB is the best, and RUC is better than NOAH. SLAB gives the lowest absolute error for area-averaged SAT, and tends to depict the western Pacific subtropical high with the easternmost position at low levels. The LSSs modify the simulated SAT, primarily via the transfer of sensible heat from the land surface to the atmosphere. The physical mechanism of the positive feedback between atmospheric circulation and the SAT is unimportant, with "negative" feedback over most of the simulated areas. This study emphasizes the importance of improving LSSs in SAT forecasting by numerical models.

WRF, land surface scheme, high-temperature weather, sensitivity experiment.

Citation: Zeng X M, Wu Z H, Xiong S Y, et al. Sensitivity of simulated short-range high-temperature weather to land surface schemes by WRF. Sci China Earth Sci, 2011, 54: 581−590, doi: 10.1007/s11430-011-4181-6

Because of global warming and other factors such as the urban heat island effects, high-temperature weather/climate events occur frequently worldwide, exerting severe effects on human health, agriculture, and transportation [1]. However, currently there is no strict definition of so-called high-temperature weather or heat waves [2]. Generally, a heat wave is defined as a weather or climate disaster with extremely high surface air temperatures (SATs), or with a prolonged period of excessively hot weather, to which it is difficult for the human body to adapt. Also, at present there is no uniform standard for heat waves. For example, the National Weather Service (NWS) of the United States considers the effects of temperature and relative humidity, and an excessive heat warning is issued by the NWS when daytime heat index values are expected to reach 40.5°C or above for two consecutive days, or when the daytime heat index is expected to exceed 46°C for any length of time [3]. In China, based on climate and environmental characteristics, daily extreme high temperature has been divided into three levels: high temperature (⩾35°C), harmful high temperature (⩾38°C), and intensely hazardous high tempera-

*Corresponding author (email: xmzen@sohu.com)

ture ($\geqslant$40°C) [4].

Land surface processes (LSPs) have substantial influences on high-temperature weather. The land surface is an important component of the climate system, and LSPs control the exchanges of various kinds of energy and substances between the land surface and the overlaying atmosphere. These interactions have received considerable attention in last several decades, which has focused on their effects on land surface hydrology and climate [5–11]. Over the past decade, effects of LSPs on short-range weather have been recognized gradually [12–16]. Solar radiation and downward longwave radiation are partitioned directly at the land surface between sensible and latent heat fluxes, and feedback to the atmosphere, whereby the SAT will be strongly influenced. Therefore, the land surface also has an important role in the evolution of SAT, land surface schemes (LSSs) in regional models will have a strong influence on simulating short-range ($\leqslant$3 days) high-temperature weather.

Numerical studies of heat waves have focused on investigations of long-term series data [17–21], and climate simulations and forecasts [22–24]. Gershunov et al. [19] analyzed the 2006 summer California-Nevada heat wave, and discussed the relative contribution of atmospheric circulation, moisture transport and other factors to the heat wave and the possible relationship between global warming and heat waves. Using a general circulation model, Wolfson et al. [22] investigated the summer 1980 United States heat wave, and indicated that higher than normal sea-surface temperature (SST) anomalies in the North Pacific (the lower than normal soil moisture anomalies over the continental United States) are unfavorable (favorable) for heat wave persistence. While the SAT is one of the most important factors in short-range research and applications with a large number of regional or global models [25–29], there is little if any literature on the sensitivity of simulated short-range high-temperature weather to LSSs. Through sensitivity analysis, we can better understand the performances of different LSSs in simulating high-temperature weather, and also be well-advised for improving of LSSs and the forecasts using these models. Therefore, examining the sensitivity of simulated high-temperature weather to different LSSs with regional models is of great importance.

At the same time, there are at least several important scientific issues requiring further in-depth studies on short-range regional high-temperature weather using the mesoscale Weather Research and Forecasting (WRF) model. These issues include:

(1) What is the performance of the WRF in simulating short-range high-temperature weather with different LSSs? As a next-generation mesoscale model WRF is one of the most representative [26–29], whose physical parameterization options have been studied mainly on the effects of simulation results for strongly convective, stormy cases [30–32]. The effects of different LSSs on extreme temperature events have yet to be incorporated in models. Holt et al. [31] examined the sensitivity of synoptically-forced convection to soil and vegetative processes including transpiration with three LSSs in the IHOP project, and indicated that detailed representation of land surface processes should be included in weather forecasting models, particularly for severe storm forecasting where local-scale information is important.

(2) What are the systematic differences between different WRF LSSs for high-temperature weather simulation? If the systematic differences are explored with different WRF LSSs for short-range weather simulation, it will greatly favor the configuration of the members of ensemble forecasting, and reduce systematic errors in ensemble forecasting [25]. However, WRF short-range sensitivity simulations on the physical options are conducted currently for temporally discontinuous cases or individual cases [30–32], from which no systematic differences can be deduced while the effects of complex physical interactions can be somewhat revealed.

(3) Concerning the mechanism of how different LSSs influence regional high-temperature weather in China, is there a mechanism difference between China and other regions? Through regional climate model simulations, Fischer et al. [24] suggested that precedent soil moisture has a significant effect on the 2003 European heat wave simulation, and that there is a positive feedback mechanism between atmospheric circulation and the SAT controlling the synoptic regime of thermal lows. Due to differences in weather and climate systems and in land surface characteristics, different regions may show differences in the nature of their land-atmosphere interactions. This would greatly improve our understanding of the nature of regional land-atmosphere interactions within some areas (e.g., southern China), and improve LSS simulation performance in researching the mechanism of how LSSs influence short-range high-temperature weather.

This study is intended to answer the above questions. We performed 24-h simulations using three LSSs in WRF to examine the sensitivity of short-range high-temperature weather simulation to the LSSs. To further reveal systematic differences between different LSSs on simulations over southern China, we chose the case of the late July 2003 heat wave to explore these systematic differences by integrating for 24 h over a 10-day time period for a single model domain (see the Subsection on experimental design). Based on the continuous 24-h simulation results, we further analyzed the mechanism of land-atmosphere interactions for the heat wave over southern China.

1 Climatologic background

The western Pacific subtropical high (WPSH) and the boreal cold air mass are the two major synoptic regimes controlling the summer monsoon system over southern China.

The WPSH displayed an extreme anomaly in the summer of 2003, while the boreal cold air mass had a relatively weak influence, which led to an exceptional heat wave over the region [20]. Figure 1(a) compares the geopotential height anomaly for July, 2003 and the climatological average, and shows the WPSH during the period with a belt-like longitudinal distribution spanning about 15° of latitude. The 5880 gpm-contour ridge extended westwards at 110°E. Compared with the climatological average, the WPSH exhibits exceptionally significant anomalies in longitudinal extent and in area, and intensity shows a positive bias with a more westward distribution for the WPSH. Figure 1(b) presents variation in July SATs over the D2 area (see Figure 2(b)), which is representative of the Yangtze-Huaihe basin and South China for the last 30 years. This suggests that July 2003 was the month with the hottest climate in southern China in recent decades.

Based on daily SAT measurements in China (not shown) the extreme high-temperature weather in summer 2003 peaked in late July. During this period, daily high temperatures (i.e., daily maximum SATs) reached 38–40°C in some areas such as the southern Yellow River and Huaihe basins, the middle and lower reaches of the Yangtze River, northern South China, east Sichuan Province, and Chongqing Municipality (Figure 2(a)). Temperatures reached 40–43°C in some regions such as central and southwest Zhejiang, north Fujian, and central Jiangxi provinces. In many regions daily maximum SATs over the same period exceeded historical records. In our study area between 26°–32°N (the southern part of the Yangtze River, and South China), daily maximum SATs of greater than 35°C occurred daily in late July. We therefore, chose late July, 2003 as the heat wave simulation period in this study.

2 Model and experimental design

We applied the mesoscale model WRF (ARW) Version 2.2. WRF is a next-generation mesoscale model developed in recent years by the National Centers for Environmental

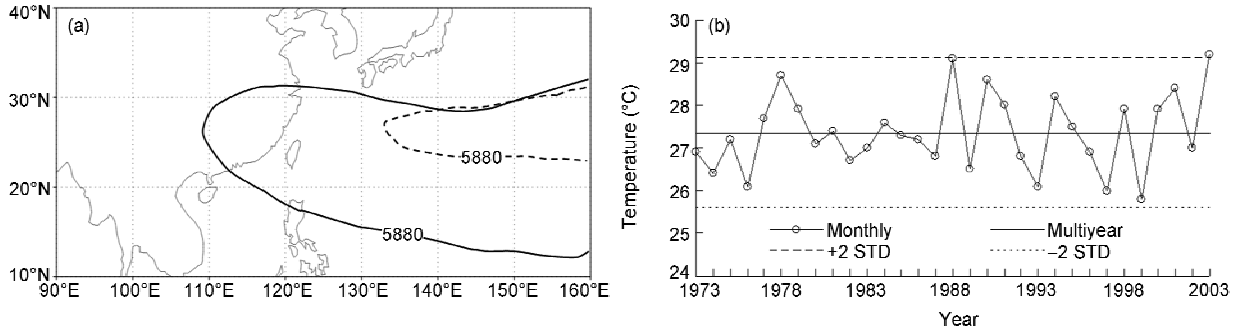

Figure 1 (a) July 5880 gpm contour at 500 hPa derived from a multiyear climatological average (1971–2000, dashed line) and from 2003 (solid line). (b) Variation in SAT over the last three decades for southern China.

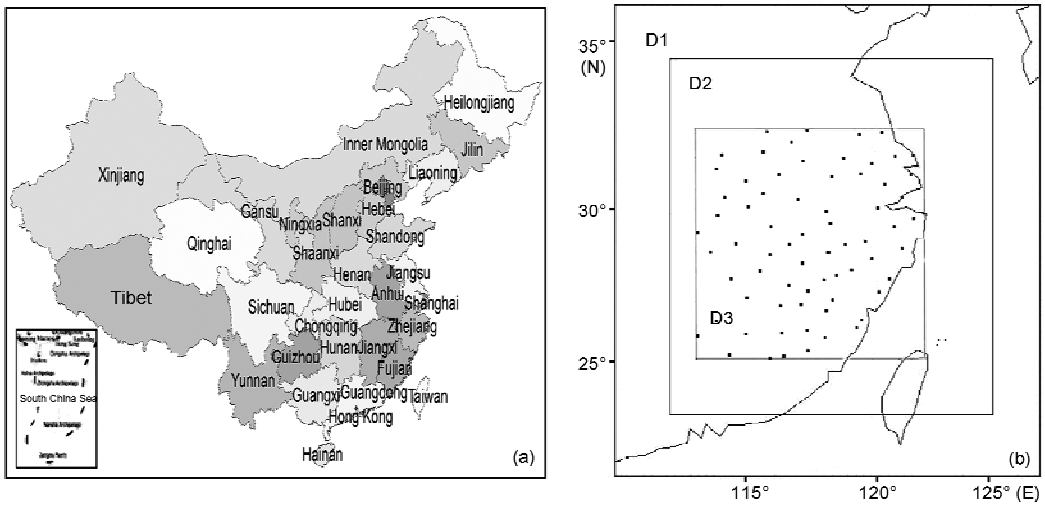

Figure 2 (a) Provinces, autonomous regions, and municipalities of China. (b) Model domain and distribution of meteorological stations used in the analysis.

Prediction (NCEP) and other research institutions [33], and has been used widely in various research and operational forecasting. It features a numerical dynamic framework, and also contains many advanced physical parameterization schemes. In this work the major physical schemes [33] include the Betts-Miller-Janjic convective parameterization, microphysics of Lin et al., MRF high-resolution boundary layer parameterization, the RRTM cloud-radiation scheme and Goddard shortwave radiation scheme, and three LSS model options (the 5-layer thermal diffusion scheme of Dudhia, NOAH LSS, and RUC LSS). All three LSSs calculate land-atmosphere exchanges of momentum, sensible heat, latent heat and radiative energy based on their methodologies for balancing energy and water. The 5-layer thermal diffusion scheme (hereafter SLAB) is used from the same module of the mesoscale model MM5 [34], its soil column is divided into five layers with the thicknesses of 1, 2, 4, 8, and 16 cm. Its energy calculation includes radiative, sensible and latent heat fluxes, which focuses on describing surface temperature variations at a high frequency and short time scales. The NOAH scheme originates from the Oregon State University (OSU) LSS [35], and has been developed continuously with the cooperation of several agencies. NOAH contains energy and hydrological process parameterizations for soil, vegetation canopy and snow cover and forecasts soil temperature and moisture for four layers (10, 30, 60, 100 cm thick). The RUC LSS is the scheme used in the NCEP operational weather service, and accounts for processes of soil, snow cover and vegetation at six layers. Through equations for surface energy and moisture balance, it computes soil temperature and moisture. In terms of relatively parameterization complexity, the SLAB scheme is simplest, the RUC LSS is the more complex, and the NOAH scheme is most complex.

We applied two-way nesting of domains in the experiments, in which the parent domain D1 (the model domain) is centered at (29°N, 118°E) with 55×62 grid points at a 30-km resolution, and the small domain D2 has 124×139 grids at a 10-km resolution (Figure 2(b)). A vertical resolution of 31 uneven levels is set with the top prescribed at 50 hPa. The following analysis involving regional averages focuses on the land surface part of the D3 domain, in which the heat wave mainly occurred, and which is within and slightly smaller than the D2 domain. Therefore, the settings of the model domain were favorable for investigations of LSS-induced effects on the simulated high-temperature weather over a relatively large area at a high resolution.

For initial and boundary conditions, NCEP 1°×1° analysis was used. The initial fields for the 24-h integrations employed analysis covering the period 12:00 UTC 20 to 12:00 UTC 29 July 2003 (the adjacent initial fields have a 24-h interval), i.e., ten 24-h integrations were conducted with a time step of 60 s. For every 24 h, the integrations were denoted according to the initial date of the integrations (e.g., the "D20" experiment). All three LSSs were applied to each integration, in which the initializations of the LSSs used the same NCEP analysis and were modified to adapt to the specific LSS.

At present, there are three kinds of the SAT forecast outputs from operational agencies: daily high and low temperatures (daily maximum and minimum SATs, respectively), and hourly SATs. Even under the same synoptic system that controls the weather, the timing of daily maximum SAT may vary over different regions because of differences in land surface and atmospheric conditions. However, in general the SAT approaches the daily maximum value at approximately 14:00 Beijing Time (BJT), when the SAT is representative of daily maximum SAT. We therefore analyzed the SAT results and related quantities with an integration length of 18 hours (i.e., 06:00 UTC, or 14:00 BJT) by different LSSs, so as to explore the sensitivity of the late July 2003 high-temperature weather simulation to the LSSs. As all the physical parameterization options are the same except for the LSSs, the differences in integration results reflect the LSS-induced effects only. Systematic differences may be revealed to some extent via thirty 24-h integrations from the three LSSs, and therefore the remainder of this paper focuses on the analysis of differences among simulation results from different LSSs.

3 Preliminary analysis of simulation results

3.1 Spatial distribution of SAT

From model results of each 24-h integration (not shown), the SAT simulation results and SATs from NCEP reanalysis are in good agreement because of the same lateral-boundary forcings of the NCEP reanalysis data. However, quite large differences from different LSSs can be identified. To explore the overall short-range performance of each LSS for simulating the high-temperature weather in late July 2003, we analyzed the average results at 14:00 BJT in which the LSSs integrations covered a period of 18 h. The SATs were close to the maximums.

Figure 3(a)–(d) shows simulated SAT distributions of 10-d averages at 14:00 BJT from the three LSSs and corresponding NCEP reanalysis fields. The three LSSs can successfully simulate SAT distributions. On average, Hunan, Jiangxi and Zhejiang provinces showed abnormally high temperatures, whereas southern and northern parts of these regions exhibited relatively lower temperatures. The distributions of SATs higher than 35°C were also reasonably simulated. There were also large differences among the LSS-induced SAT results. For SATs higher than 38°C, RUC produces the maximum area, and reproduces best the positions and intensities of the two major centers at 28.4°N (the center located at 113°E is referred to as the "west" one, with the "east" one at 117°E), with the position biases slightly to the west. SLAB simulates quite well the location and intensity of the "west" center but fails to reproduce the

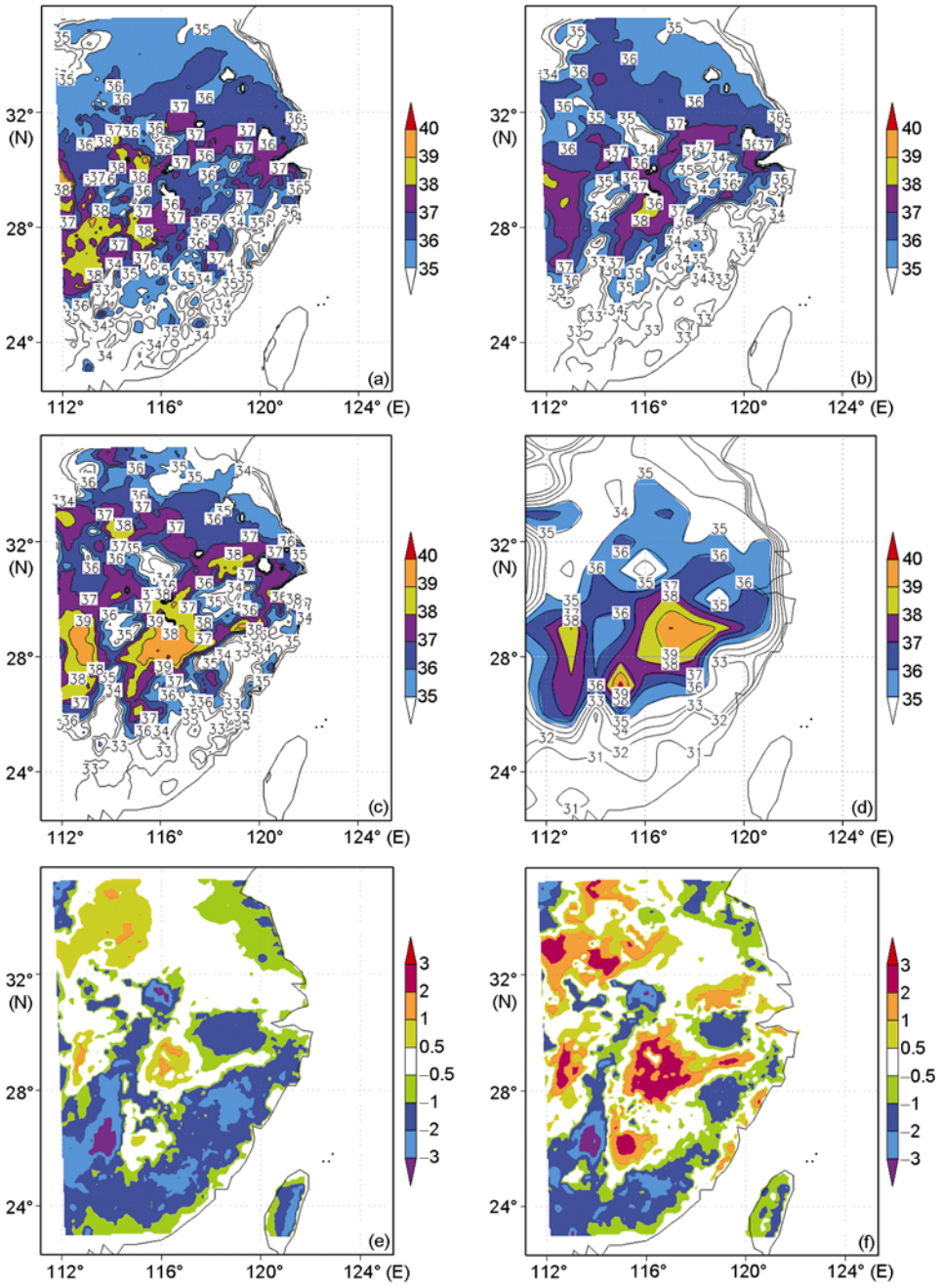

Figure 3 Ten-d mean SAT distributions at 14:00 BJT. (a) SLAB; (b) NOAH; (c) RUC; (d) NCEP reanalysis; (e) NOAH-SLAB; (f) RUC-SLAB. Unit: °C.

"east" one (Figure 3(a)), and compared to RUC exhibits SATs 1–2°C higher in the southern coastal part of the model domain and generally lower SATs elsewhere (Figure 3(f)). NOAH fails to capture SATs higher than 39°C (Figure 3(b)), with its centers lower than those generated by SLAB (Figure 3(e)). Between the three LSSs, the maximum point SAT differences can be greater than 6°C (i.e., RUC-SLAB). Therefore, in terms of the simulation for SATs higher than 35°C, RUC is the best, SLAB is the second best, and NOAH is the worst. In addition, high-temperature areas from different LSSs show large differences in intensity.

3.2 Assessments with the measures

We take *NA* as the number of stations for which the high SATs (i.e., over 35°C here) are correctly simulated, *NB* the number of stations with simulated high SATs where lows were observed, and *NC* for stations simulated low SATs yet with observed highs. Hence, we can assess the three LSSs using a threat score (*TS*) for the stations, which is computed as [29]

$$TS=NA/(NA+NB+NC). \quad (1)$$

In current Chinese meteorological agencies, this *TS* algo-

rithm for SAT is applied widely in medium- and short-range weather forecast for quality inspection. The TS only reflects a successful ratio when there is a hot-weather event. When the simulated high-temperature area completely coincides with the observed, *TS*=1, suggesting a completely correct simulation, and the simulation is poorer the nearer *TS* is to 0.

In addition, we used the average absolute error (*ABE*) and root-mean square error (*RMSE*) for evaluation:

$$ABE = \frac{1}{N}\sum_{i=1}^{N}|P_i - O_i|, \tag{2}$$

$$RMSE = \sqrt{\frac{1}{N}\sum_{i=1}^{N}(P_i - O_i)^2}, \tag{3}$$

where P_i and O_i are forecast and observed SATs for the ith station (see Figure 2 for the location of the 74 stations used).

Figure 4 shows results of the TS (for SATs$\geqslant$35°C) and errors for each 24-h integration with the three LSSs at 14:00 BJT over the D3 domain. As shown in Figure 4(a), for each integration SLAB presents the highest TS of ~0.4 (with a maximum of 0.64), RUC presents a lower TS compared with SLAB, and NOAH produces minimums. Between SLAB and NOAH there is generally a TS difference of ~0.2 for individual late July days. There was a maximum difference of ~0.3 (the D25 experiment) that also had a relative amplitude over 100% (relative to the small TS value from NOAH). These results illustrate that a more suitable LSS can lead to better simulations of the high-temperature field, but also exhibit very large differences in the TS because of different LSSs.

Generally, the three LSS-induced errors were slightly lower than those in the short-range forecast for North American (i.e., >5°C) [29] (Figure 4(b), (c)) SLAB had the least error, RUC presented a larger error, and NOAH produced the largest. This is consistent with the TS results. In addition, RUC and NOAH differed little in the errors, while both deviate to quite an extent from SLAB with an average ABE difference of ~0.5°C and a maximum of ~1.0°C. This further illustrates that using an appropriate LSS can reduce to a large extent the errors in regional simulations of high temperatures.

4 Analysis of the mechanism

The above-mentioned results show large LSS-induced differences in the SAT simulation. From the point of view of the physical mechanism, these differences are induced primarily by different land surface fluxes from different LSSs, in which land surface sensible heat is transported upwards and directly heats the surface layer atmosphere, exerting a critical influence on SAT. Meanwhile, because of the little effect of moist hot weather convection during the simulation period, surface latent heat played a secondary role in affecting the SAT. Figure 5 shows the temporal variations in area-averaged sensible heat and latent heat fluxes from different LSSs for the 10-d integrations. Although during the nights the heat fluxes were extremely small, LSS-induced differences were still quite large and peaked at 06:00 UTC (14:00 BJT) (Figure 5(a), (b)). RUC showed superiority in

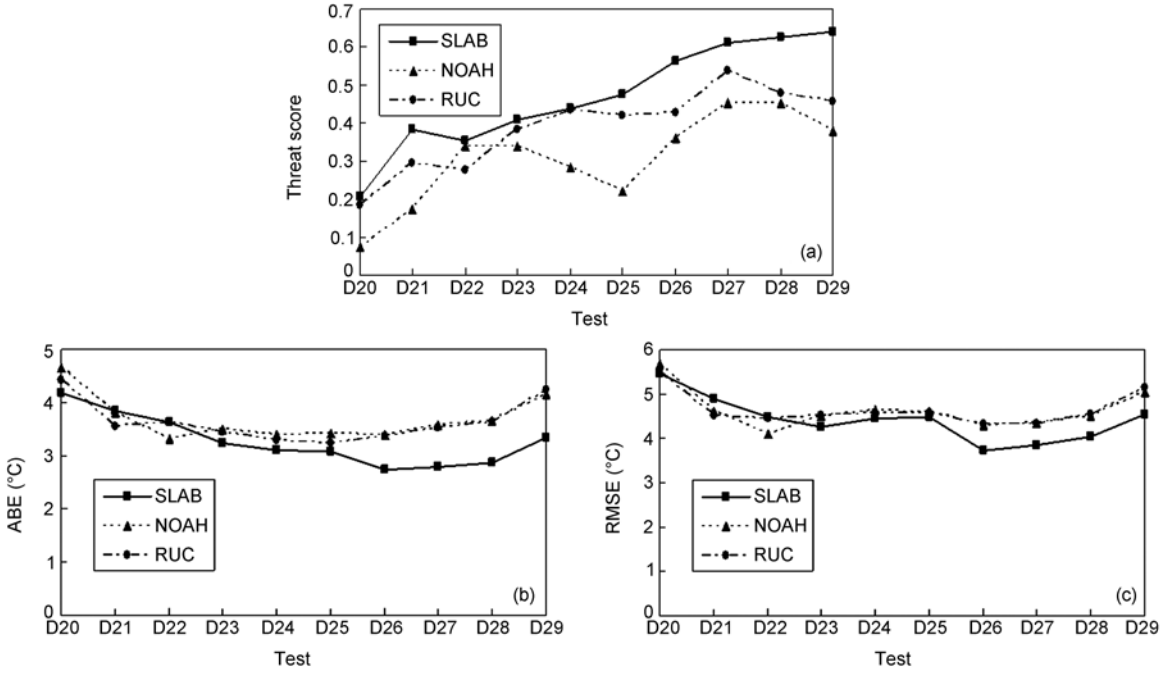

Figure 4 SAT results over the D3 domain.

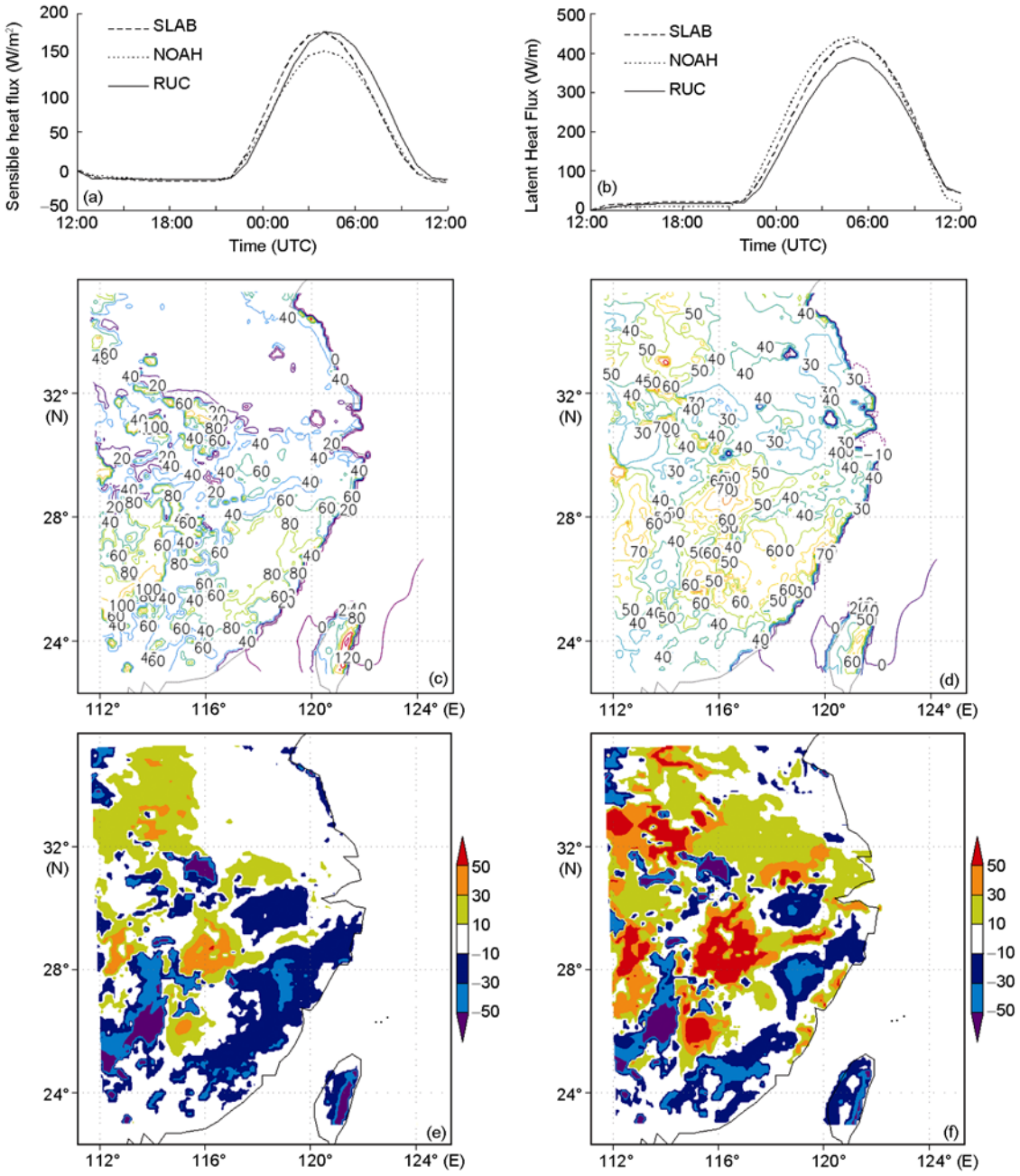

Figure 5 Area-averaged sensible and latent heat fluxes from the 10 d, 24-h integrations (Units:w/m^2). (a) Diurnal variation in sensible heat flux; (b) diurnal variation in latent heat flux; (c) SLAB distribution of sensible heat flux; (d) NOAH distribution of sensible heat flux; (e) NOAH minus SLAB distribution of sensible heat flux; (f) RUC minus SLAB distribution of sensible heat flux.

simulating SATs $\geqslant$38°C, as mentioned above, and this is closely related with its higher sensible heat flux and lower latent heat flux. Comparing Figure 5(e) with 5(f) shows that RUC simulated higher sensible heat flux than NOAH, which led to a higher SAT from RUC (Figure 3). Comparing Figure 3(e)–(f) with 5(e)–(f), there is a clear similarity between the distribution of enhanced (reduced) sensible heat flux and that of the increased (decreased) SAT. These suggest that different LSS-induced sensible heats are dominantly responsible for SAT change, which is consistent with the results of a previous study showing that different land-atmosphere interactions (e.g., between different soil moistures and atmosphere) result in different SATs via surface fluxes [24].

The western Pacific subtropical high (WPSH) is one of the crucial regimes controlling the summer weather and climate of China. Wu et al. [36] pointed out that the latent heating of condensation is a critical factor determining the position and intensity of the WPSH in summer in the eastern hemisphere. Zhou et al. [37] suggested that increased

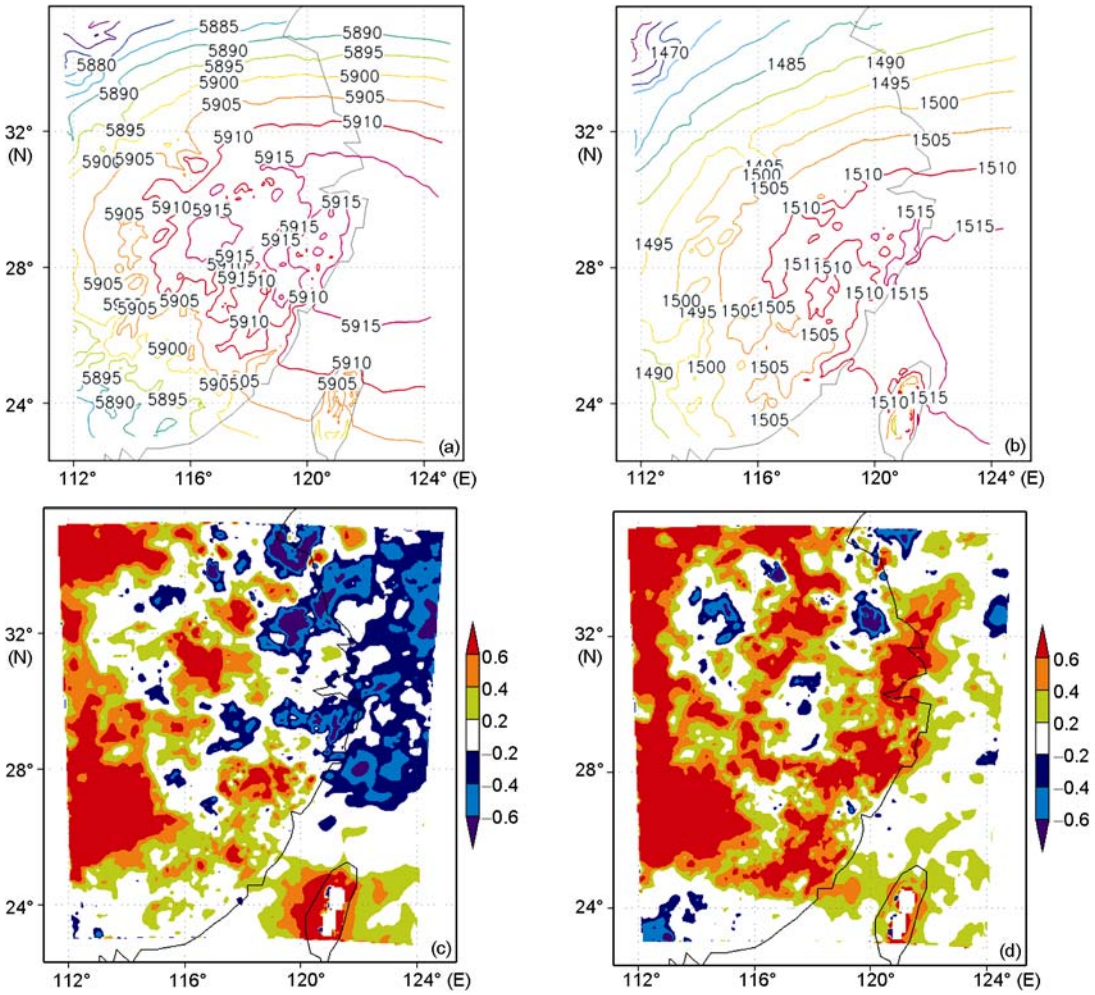

Figure 6 Area-averaged 500 hPa and 850 hPa geopotential heights at 14:00 BJT from the 10 d, 24-h integrations (Units: gpm). (a) SLAB 500 hPa; (b) SLAB 850 hPa; (c) NOAH-SLAB 850 hPa; (d) RUC-SLAB 850 hPa.

convective heating in the equatorial Indian Ocean, associated with the Earth's surface non-uniform heating, is one of the reasons for the western extension of the WPSH. Different LSSs result in differences in land surface moisture and energy transfers, and in dynamical and thermal structures of the atmosphere which also influences simulated WPSH activity. Many researchers have investigated the mechanism of how the 2003 heat wave in southern China originated and was maintained, and generally concluded that an exceptionally strong WPSH and its prolonged duration are mostly responsible [20, 21]. Constrained by the law of air mass conservation, air mass convergence in the upper layer of the troposphere occurs within the WPSH and there is divergence in the lower layer, which correspondingly leads to the adiabatic sinking of the air and further affects low-level temperature. Factors affecting the WPSH features will have an effect on the SAT.

The WPSH controlled the climate in July 2003 over the study area, shown by 500 and 850 hPa geopotential height results averaged over the period (Figure 6(a)–(b)). At the low level of 850 hPa, NOAH and RUC simulate slightly stronger WPSHs with a slightly western extension compared with SLAB, and RUC shows the strongest WPSH of the three LSSs (Figure 6(c)–(d)). The intensified low-level circulation also leads to a stronger heating effect of the sinking air on the low-level temperature, and facilitates SAT increase (theoretically, there exists a positive feedback between atmospheric circulation and SAT). However, comparing Figure 6(c)–(d) with 3(e)–(f) shows clearly that over most of the simulated land surface area (24°–32°N) SAT distribution decrease (increase) corresponds well to that of increase (decrease) in the 850 hPa geopotential height, i.e., there is a negative feedback for the area. Theoretically, it is apparent that the change from SLAB to NOAH (or RUC) would cause the positive feedback between circulation and temperature changes, but most simulated areas exhibit a negative feedback. This indicates that the temperature effect induced by the low-level circulation changes is of secondary importance. By comparing Figure 3(e)–(f) with 6(e)–(f), and Figure 3(e)–(f) with Figure

6(c)–(d), the similarity between distributions of changes in sensible heat and in the SAT is clearly higher than the similarity between those of atmospheric circulation and the SAT, The areas near the northern and southern boundaries indicate no above-mentioned relation for the areas (or the present relation here is opposite to the positive feedback). This further explains that for the main high-temperature area, the simulated SAT change was induced by surface sensible heat flux rather than by atmospheric circulation. Using a regional climate model to investigate land-atmosphere interactions in the European heat wave event of the summer, 2003, Fischer et al. [24] suggested that drier land surfaces favor the generation of thermal pressure low which intensifies the ridge of a mid-troposphere high. Hence, there is a mechanism of positive feedback between atmospheric circulation and low-level temperature. Our study, however, indicates that positive feedback is not important for the synoptic regime of the WPSH (as is of the dynamical type) using simulations in the short-range weather mode. Over the study area, the "negative" feedback mechanism dominates.

5 Concluding remarks

We employed three LSSs in the mesoscale model WRFV2.2 to simulate high-temperature weather occurring in late July 2003 over South China and southern Yangtze River areas. For each LSS, 24-h integrations have been performed for 10 consecutive days. Our major conclusions are as follows:

(1) The distribution of surface air temperature (SAT) over the region was reproduced successfully with the three LSSs. Overall, the simulated high-temperature weather was sensitive to the LSSs. In terms of threat score (*TS*) for SATs higher than 35°C at 14:00 BJT, SLAB was the best over the region, RUC the next best, and NOAH was the worst with large *TS* differences between different LSSs (e.g., in the 10 integrations, the TS differences among different LSSs were generally ~0.2, and the largest *TS* difference reached 0.3). Error analysis also showed that different LSSs can result in large differences in errors, with the smallest error from SLAB and close results from RUC and NOAH. It is noteworthy that RUC better simulated the distribution of harmful SATs higher than 38°C, although it had poorer results for the TSs higher than 35°C and error analysis.

(2) In terms of the mechanism by which the LSSs affect simulated SATs over the region, the simulated SAT differences are by directly induced LSS differences in sensible heat flux. Surface sensible heat flux can result in changes in atmospheric circulation for the simulated western Pacific subtropical high (WPSH). At the 850 hPa level, the strongest influence was by RUC, was less strong for NOAH, and weakest for SLAB. A previous study of the 2003 European heat wave showed positive feedback between circulation change (as induced by different soil moisture) and surface temperature change [24]. For the controlling synoptic regime of the WPSH, which is the dynamical type over the region studied here, a positive feedback mechanism between LSS-induced circulation change and SAT change is not important, or there instead exists "negative" feedback over the main high-temperature area.

(3) It is relatively easy to examine LSS-induced systematic differences for short-range simulations based on the experimental design used here (i.e., 30 integrations with a 24-h time period over a prescribed study domain for the late July, 2003 heat wave). RUC gives the best simulation for the distribution of >38°C SATs, while SLAB produces the lowest averaged absolute errors and gives the easternmost lower-level WPSH ridges. These systematic differences are important for understanding the performance of the mesoscale model, for improving model performance with the LSSs as submodules for simulations and applications, and for enhancing numerical SAT prediction.

It should be also noted that the so-called "different LSS effects" is a generalization. The simulated differences actually represent the effects of both initial values of LSS parameters (e.g., different initial soil temperatures according to different soil column layering) and from parameterizations (e.g., different algorithms for vegetation effects). The above-mentioned LSS-induced systematic differences are obtained under specific model settings, suggesting that systematic differences may reflect general features of the WRF-simulated heat waves under the model configuration. However, land-atmosphere interactions may differ to a large extent between geographic regions and from synoptic regimes, and simulation results of sensitivity to LSSs are related to factors such as model domain size, treatment of lateral boundaries, and physical options, among others. It is advisable for users of the models to test fully against these aspects before model application.

In addition, it is necessary to be clear that for regional model simulations, results are determined by initial and boundary conditions, and internal dynamical and physical processes, and that the choosing of model domain and the positioning of the lateral boundaries may have substantial influence on simulations. Although we designed the experiments to reveal the effects of LSSs at relatively high resolutions and to discuss different LSS-induced effects on a relatively large land area, because of our limited computational resources, the lateral boundary of the D1 domain in our study was close to that of the D2 subarea. If a greater distance between these two lateral boundaries had been set, the effects from NCEP data-induced lateral boundaries would have been reduced to some extent. Another limitation of this work lies in the period of time for the short-range integrations. The simulations were done over 24 h, the main investigated period of time was 18 h for the high-temperature weather, and the time of land-surface effects on the atmosphere is longer. If we had compared these results with those from other periods of time, e.g., 36 h, it would have shown more results favorable to investigating short-range

LSS-induced effects. With improved computational resources and model performance, these deficiencies can be overcome in the follow-up studies.

The authors would like to thank two anonymous reviewers for helpful advice on this paper. The data for this study are from the Research Data Archive (RDA) which is maintained by the Computational and Information Systems Laboratory (CISL) at the National Center for Atmospheric Research (NCAR). NCAR is sponsored by the National Science Foundation (NSF). The original data are available from the RDA (http://dss.ucar.edu) in dataset number ds083.0. The analyses were prepared by the National Centers for Environmental Prediction (NCEP). This work was supported by National Natural Science Foundation of China (Grant No. 40875067) and in part by Knowledge Innovation Program of the Chinese Academy of Sciences (Grant No. IAP09306).

1 Stott P A, Stone D A, Allen M R. Human contribution to the European heat wave of 2003. Nature, 2004, 432: 610–614
2 Robinson J P. On the definition of a heat wave. J Appl Meteor, 2001, 40: 762–775
3 Kalkstein S L, Jamason P F, Greene J S, et al. The Philadelphia hot weather-health watch/warning system: Development and application, summer 1995. Bull Amer Meteorol Soc, 1996, 77: 1519–1528
4 Zhang S Y, Song Y L, Zhang D K, et al. Climatic characteristics of summer high temperature and assessment methods in the large cities of North China. J Geogr Sci, 2006, 16: 13–22
5 Manabe S. Climate and ocean circulation. Part I: The atmospheric circulation and the hydrology of earth's surface. Mon Weather Rev, 1969, 97: 740–774
6 Giorgi F, Marinucci M R. Validation of regional climate model over Europe: sensitivities of wintertime and summer time simulations to selected parameterizations and lower boundary conditions. Q J R Meteorol Soc, 1991, 117: 1171–1206
7 Zeng X M, Zhao M, Yu R C, et al. Application of a "big-tree" model to regional climate modeling: A sensitivity study. Theor Appl Climatol, 2003, 76: 203–218
8 Li Q, Sun S F. Development of the universal and simplified soil model coupling heat and water transport. Sci China Ser D-Earth Sci, 2008, 51: 88–102
9 Tian X J, Xie Z H. A land surface soil moisture data assimilation framework in consideration of the model subgrid-scale heterogeneity and soil water thawing and freezing. Sci China Ser D-Earth Sci, 2008, 51: 992–1000
10 Zhang Q, Hu X J, Wang S, et al. Some technological and scientific issues about the experimental study of land surface processes in Chinese Loess Plateau (LOPEX). Adv Earth Sci, 2009, 24: 363–372
11 Zeng X M, Liu J B, Ma Z G, et al. Study on the effects of land surface heterogeneities in temperature and moisture on annual scale regional climate simulation. Adv Atmos Sci, 2010, 27: 151–163
12 Pielke R A. Influence of the spatial distribution of vegetation and soils on the prediction of cumulus convective rainfall. Rev Geophys, 2001, 39: 151–177
13 Zeng X M, Zhao M, Su B K. A numerical study on effects of land-surface heterogeneity from 'Combined Approach' on atmospheric process. Part II: coupling-model simulations. Adv Atmos Sci, 2000, 17: 441–455
14 Zhang C L, Miao S G, Li Q C, et al. Impacts of fine-resolution land use information of Beijing on a summer severe rainfall simulation (in Chinese). Chin J Geophys, 2007, 50: 1373–1382
15 Trier S B, Chen F, Manning K W, et al. Sensitivity of the PBL and precipitation in 12-Day simulations of warm-season convection using different land surface models and soil wetness conditions. Mon Weather Rev, 2008, 136: 2321–2343
16 Zeng X M, Zhang Q. Numerical study of the effects of disturbances of land surface parameters on the simulation of a heavy rainfall over Northwest China (in Chinese). Sci Meteorol Sin, 2009, 29: 291–298
17 Brunetti M, Buffoni L, Mangianti F, et al. Temperature precipitation and extreme events during the last century in Italy. Glob Planet Change, 2004, 40: 141–149
18 Zhai P, Pan X. Trends in temperature extremes during 1951–1999 in China. Geophys Res Lett, 2003, 30: 1913, doi: 10.1029/2003GL018004
19 Gershunov A, Cayan D R, Iacobellis S F. The great 2006 heat wave over California and Nevada: Signal of an increasing trend. J Clim, 2009, 22: 6181–6203
20 Lin J, Bi B G, He J H. Physical mechanism responsible for western Pacific subtropical high variation and hot wave in Southern China in July 2003 (in Chinese). Chin J Atmos Sci, 2005, 29: 594–599
21 Yang H, Li C Y. Diagnostic study of serious high temperature over South China in 2003 summer (in Chinese). Clim Environ Res, 2005, 10: 81-85
22 Wolfson N, Atlas R, Sud Y. Numerical experiments related to the summer 1980 U.S. heat wave. Mon Weather Rev, 1987, 115: 1345–1357
23 Kharin V V, Zwiers F W, Zhang X, et al. Changes in temperature and precipitation extremes in the IPCC ensemble of global coupled model simulations. J Clim, 2007, 20: 1419–1444
24 Fischer M E, Seneviratne S I, Vidale P L, et al. Soil moisture-atmosphere interactions during the 2003 European summer heat wave. J Clim, 2007, 20: 5081–5099
25 McCollor D, Stull R. Evaluation of probabilistic medium-range temperature forecasts from the North American Ensemble Forecast System. Weather Forecast, 2009, 24: 3–17
26 Cheng W Y Y, Steenburgh W J. Evaluation of surface sensible weather forecasts by the WRF and the Eta models over the western United States. Weather Forecast, 2005, 20: 812–821
27 Wegiel J, LaCroix K, Rugg S, et al. Operational implementation of the Weather Research and Forecasting (WRF) system at the Air Force Weather Agency. 6th WRF Users' Workshop. National Center for Atmospheric Research, Boulder, CO, June 27–30, 2005
28 Mölders N. Suitability of the Weather Research and Forecasting (WRF) model to predict the June 2005 fire weather for interior Alaska. Weather Forecast, 2008, 23: 953–973
29 Etherton B, Santos P. Sensitivity of WRF forecasts for South Florida to initial conditions. Weather Forecast, 2008, 23: 725–740
30 Jankov I, Gallus J W A, Segal M, et al. The impact of different WRF model physical parameterizations and their interactions on warm season MCS rainfall. Weather Forecast, 2005, 20: 1048–1060
31 Holt T R, Niyogi D, Chen F, et al. Effect of land-atmosphere interactions on the IHOP 24–25 May 2002 convection case. Mon Weather Rev, 2006, 134: 113–133
32 Ha H K, Wang Z H, Kim J Y, et al. The impact of cumulus parameterizations and micro-physics schemes of different combinations on typhoon track prediction (in Chinese). J Tropical Meteorol, 2009, 25: 435–441
33 Skamarock W C, Klemp J B, Dudhia J, et al. A description of the Advanced Research WRF Version 2. NCAR Technical Note NCAR/TN-468+STR. National Center for Atmospheric Research, 2005
34 Grell A G, Dudhia J, Stauffer D R. A description of the fifth generation Penn State/NCAR Mesoscale Model (MM5). NCAR Technical Note NCAR/TN-398+STR. National Center for Atmospheric Research, 1995
35 Ek M B, Mitchell K E, Lin Y, et al. Implementation of Noah land-surface model advances in the National Center Environment Prediction operational mesoscale Eta model. J Geophys Res, 2003, 108(D22): 8851, doi: 10.1029/2002JD003296
36 Wu G X, Liu Y M, Liu P. The effect of spatially nonuniform heating on the formation and variation of sub tropical high I: Scale analysis (in Chinese). Acta Meteorol Sin, 1999, 57: 257–263
37 Zhou T, Yu R, Zhang J, et al. Why the western Pacific subtropical high has extended westward since the late 1970s. J Clim, 2009, 22: 2199–2215